Impact of theoretical priors in cosmological analyses: The case of single field quintessence

Simone Peirone,[1] Matteo Martinelli,[1] Marco Raveri,[2,1] and Alessandra Silvestri[1]

[1]*Institute Lorentz, Leiden University, P.O. Box 9506, Leiden 2300 RA, Netherlands*
[2]*Kavli Institute for Cosmological Physics, Enrico Fermi Institute,*
University of Chicago, Chicago, Illinois 60637, USA

We investigate the impact of general conditions of theoretical stability and cosmological viability on dynamical dark energy models. As a powerful example, we study whether minimally coupled, single field quintessence models that are safe from ghost instabilities, can source the Chevallier-Polarski-Linder (CPL) expansion history recently shown to be mildly favored by a combination of cosmic microwave background (Planck) and weak lensing (KiDS) data. We find that in their most conservative form, the theoretical conditions impact the analysis in such a way that smooth single field quintessence becomes significantly disfavored with respect to the standard ΛCDM cosmological model. This is due to the fact that these conditions cut a significant portion of the (w_0, w_a) parameter space for CPL, in particular, eliminating the region that would be favored by weak lensing data. Within the scenario of a smooth dynamical dark energy parametrized with CPL, weak lensing data favors a region that would require multiple fields to ensure gravitational stability.

I. INTRODUCTION

Recent observational results from weak lensing experiments [1,2] have been found to be in discordance with cosmic microwave background (CMB) measurements from Planck [3]. This discordance is usually quantified by means of consistency tests [4–7] or in terms of the $S_8 = \sigma_8 \sqrt{\Omega_m/0.3}$ derived parameter, with Ω_m quantifying the matter density and σ_8 the amplitude of the linear matter power spectrum on 8 h^{-1} Mpc scales, to which weak lensing surveys are expected to be particularly sensitive [8]. In the case of the weak lensing Kilo Degree Survey (KiDS), this discordance is measured to be at the level of 2.3σ [2].

Despite significant effort in investigating the effects of systematics on the measurements of both weak lensing [2,7,8] and Planck [9], no relevant reduction of the tension has been found so far,[1] prompting some initial investigations on whether this discordance could be due to the assumption of the standard cosmological model, ΛCDM [12,13]. In [8], the KiDS Collaboration revisited the tensions between the data sets within some simple extensions of the ΛCDM model. They found a dynamical dark energy (DE) with a time-varying equation of state to alleviate the tension, reducing it to S_8 to 0.91σ on S_8, *and* to be favored by the combined KiDS and Planck data sets, from a Bayesian model selection point of view [8].

Given this interesting result, in this paper, we investigate how connecting a *theoretically viable* DE model with the phenomenological parametrization used to perform this analysis will affect the results. In practice, we ask ourselves which *theoretically viable* DE model could correspond to the expansion history preferred by the combination of KiDS and Planck data. We shall show that the implementation of conditions of theoretical consistency inside the analysis pipeline, in the form of viability priors, allows us to answer such questions in a straighforward way; more generally, it allows us to perform theoretically informed data analysis in a very efficient way. For a previous investigation of the impact of prior information in quintessence studies, see [14].

The paper is organized as follows. In Sec. II, we revisit general conditions of stability for DE models, focusing on minimally coupled quintessence. We then describe how we implement these conditions in our exploration of Chevallier-Polarski-Linder (CPL) models. In Sec. III, we describe the data sets that we employ and, finally, we show the results of our analysis in Sec. IV. We draw our Conclusions in Sec. V.

II. DYNAMICAL DARK ENERGY: STABILITY AND VIABILITY CONDITIONS

In the analysis of observational data, it is often useful to explore broad classes of models through a framework that parametrizes the relevant deviations from the standard ΛCDM cosmological model. This approach is commonly applied to the investigation of dynamical DE models, where the equation of state is often described by the Chevallier-Polarski-Linder parametrization [15,16],

$$w_{\text{DE}}(a) = w_0 + w_a(1-a). \tag{1}$$

---

[1]We point out that other recent analysis of the KiDS data [10,11] yield different degrees of tension with Planck. Our results, however, would not be qualitatively affected by these.

When going beyond background probes, the latter is commonly combined with the parametrized post-Friedmann (PPF) framework for DE perturbations, introduced in [17–19] and implemented in the Einstein-Boltzmann solver CAMB [19]. This offers a stable and accurate description of DE perturbations over the entire parameter space of CPL, provided that the DE field remains smooth with respect to matter on the scales of interest. This is the approach used also in [8], where they found a best fit point in the third quadrant of the (w_0, w_a) plane, corresponding to a w that was below -1 in the recent past.

While adopting a parametrized framework, it is informative to make contact with known theories and associate different regions of the parameter space to different viable classes of theories. It is known that a single field, minimally coupled quintessence has to have $w > -1$ in order to be stable. When adopting the CPL parameterization, its (w0, wa) are therefore restricted to regions corresponding to $w > -1$. Outside of that range, results need to be interpreted within the realm of multifield DE. In the following, we will include these theoretical priors in the statistical analysis pipeline; this will allow us to perform parameter estimation and model selection automatically accounting for the restrictions that theoretical considerations apply on the parameter space volume.

Minimally coupled, single field models with a speed of sound equal to unity, are arguably the simplest models of dynamical DE. We will refer to them as *standard quintessence*. For these models, the DE field remains smooth on subhorizon scales, and PPF offers an accurate prescription. However, in this case, one should be careful with the allowed regions of the parameter space (w_0, w_a). Indeed, these models would generally suffer from ghost instabilities for $w < -1$ [20–23]. These instabilities arise from the wrong sign of the kinetic term, which translates into an Hamiltonian unbounded from below and, thus, into an unstable quantum vacuum. Correspondingly, $w = -1$ is referred to as the *phantom divide*, and single field models crossing through it are gravitationally unstable.

As explored in [24], while it is difficult, it is not impossible to have a quintessence model with $w < -1$, which is *effectively* stable; i.e., the rate of the instabilities is longer than the time scale of interest for the analysis. We keep this option open in our analysis; however, we will see that requiring that no instabilities develop over the relevant time interval will still cut a significant portion of the $w < -1$ region.

Alternatively, single field DE models could safely cross the phantom divide if the DE field is nonminimally coupled to gravity [25], there is kinetically braiding, i.e., mixing of the kinetic terms of the metric and the scalar [26,27], or the model includes higher order derivative operators, as discussed in [20]. However, in the former two cases, the DE component would be clustering, and in the latter case, as shown in [20], stability requires that in the region $w < -1$ the DE field behaves like a k-essence fluid with an

approximately zero speed of sound. As such, in all these cases, the DE component cannot be considered smooth on the scales of relevance for large scale structure surveys, and hence, the PPF framework does not apply. Which models could then correspond to a DE which gives a CPL history which crosses the phantom divide, while remaining relatively smooth with respect to matter (so that PPF is an accurate prescription)? As discussed in [28,29], one necessarily needs to dwell into the multifield scenarios, with additional degrees of freedom ensuring gravitational stability. This is the assumption at the heart of the PPF approach.

In this paper, we shall asses the importance of stability requirements and their impact on the results obtained with the CPL parametrization, by performing the same analysis of [8] within the realm of standard (single field) quintessence. This will allow us to show that, as expected, the model favored by data in [8] cannot correspond to such a scenario, and more importantly, if one restricts the CPL parameter space to this class of models, then ΛCDM remains a better fit to the combined data. Thus, the result of [8] should be interpreted in terms of multiple fields DE, highlighting the relevance of sound theoretical conditions when connecting viable models to purely phenomenological approaches.

To this extent, we do not employ the PPF approach of CAMB, but rather use the minimal implementation of CPL in EFTCAMB [30,31], which corresponds to a designer standard quintessence with a CPL expansion history. EFTCAMB has a stability module which imposes two sets of theoretically motivated conditions: mathematical stability conditions (MC) and physical stability conditions (PC). The former are general conditions which do not rely on any assumption connected to a specific theoretical model, but rather ensure mathematical consistency and numerical stability of perturbations in the DE sector. They include conditions for: the well-posedness of the scalar field perturbations initial value problem; the avoidance of exponential growth of the perturbations; the existence of a viable cosmological background with matter and radiation eras and an accelerated phase ($w_{DE} < -1/3$).

On the other hand, PC enforce the absence of ghost and gradient instabilities. Since we put ourselves in the case of a CPL standard quintessence, the stability check will automatically ensure that we do not explore regions of (w_0, w_a) that would correspond to an unstable model.

While MC and PC can be turned on and off independently, in our analysis, we use either MC or the full combination of the two (FC), in order to provide a full protection against instabilities. We stress that a more complete set of PC, e.g., including no-tachyon conditions [32], is being worked out.

In Fig. 1, we show the effect of MC and FC on the CPL parameter space, (w_0, w_a). As we can see in panel (a) MC prohibit the crossing of $w = -1$, cutting a relevant portion of parameter space. On the other hand, as shown in panel (b), the only cut introduced by PC is the one coming from
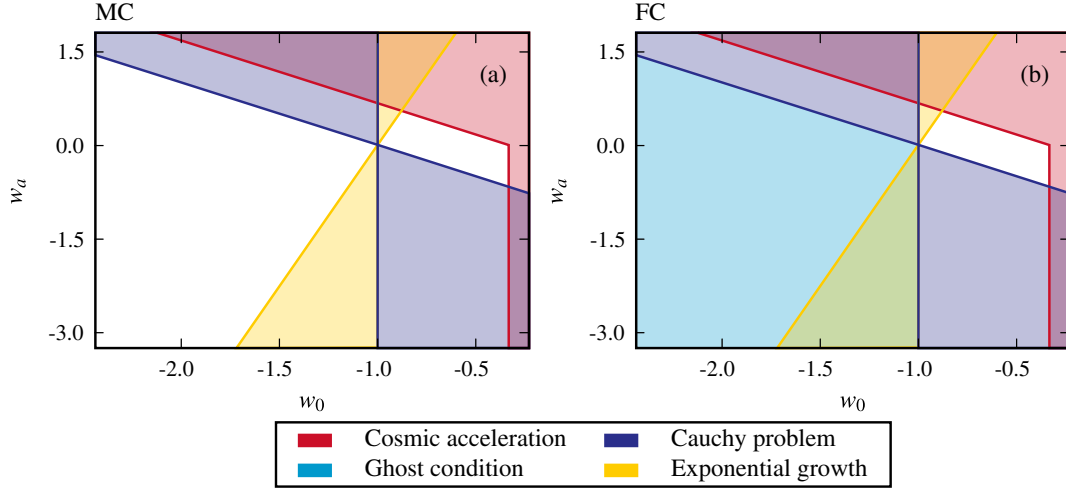
FIG. 1. Viable and nonaccessible regions of the CPL parameter space within the realm of *standard quintessence*. Different colors correspond to different viability and stability conditions, as shown in legend. In the *left* panel, we show the effects of mathematical conditions (MC), and in the *right* one, we show the full combination (FC) of mathematical and physical conditions.

the no-ghost condition, which cuts the portion of the parameter space corresponding to $w < -1$ at all times. Comparing the two panels, we can see that MC allow some parts of the $w < -1$ region, namely, those for which the instabilities are still there (from the theoretical point of view), but do not affect the observables; i.e., they do not develop over the relevant time range.

In this paper, we compare our results for CPL quintessence under MC and FC, with those of [8], where the PPF module was used. The results of our analysis will show how much impact MC and FC can have on the final results and will serve us as an example to stress the power of theoretical stability and viability conditions in the analysis of cosmological data.

III. DATA ANALYSIS

Following [8], we consider the full set of data from the tomographic weak gravitational lensing analysis of ~ 450 deg^2 by the four-band imaging Kilo Degree Survey (KiDS) [2,33,34], including Baryonic effects in the nonlinear matter power spectrum with HMCODE [35]. In addition, we also consider the Planck measurements [9,36] of CMB temperature and polarization on large angular scales, limited to multipoles $\ell \leq 29$ (low-ℓ TEB likelihood) and the CMB temperature on smaller angular scales (PLIK TT likelihood).[2]

We use EFTCAMB and EFTCOSMOMC [30,31] patches of CAMB/CosmoMC codes [38,39], and we implement these in the version of CosmoMC made publicly available by the

KiDS Collaboration [8]. We analyze KiDS and Planck both separately and combining them, sampling the standard cosmological parameters, i.e., the baryon and cold dark matter energy densities $\Omega_b h^2$ and $\Omega_c h^2$, the optical depth at reionization τ, the amplitude and tilt of primordial power spectrum $\ln 10^{10} A_s$ and n_s, and the angular size of the sound horizon at last scattering surface θ. To these we add the CPL parameters w_0 and w_a when we analyze the extension to the ΛCDM model, and we perform this analysis both in the MC and FC cases.

We adopt flat priors on the sampled parameters, using the same prior ranges defined in Table 1 of [8].

In order to assess the effect of the conditions on the possibility of reducing the low-high redshift tension with a dynamical dark energy, we exploit the same statistical tools used in [8]; this will allow us to compare our results to the standard PPF treatment of a dynamical dark energy. We therefore consider the tension between Planck (P) and KiDS (K) data sets on the $S_8 = \sigma_8 \sqrt{\Omega_m/0.3}$ parameter, defining it as

$$T(S_8) = \frac{|S_8^P - S_8^K|}{\sqrt{\sigma^2(S_8^P) + \sigma^2(S_8^K)}}. \tag{2}$$

We also assess the preference of the data for any of the considered models over ΛCDM computing the *deviance information criterion* (DIC) [40],

$$\mathrm{DIC} \equiv \chi_{\mathrm{eff}}^2(\hat{\theta}) + 2p_D, \tag{3}$$

with $\chi_{\mathrm{eff}}^2(\hat{\theta}) = -2\ln\mathcal{L}(\hat{\theta})$, $\hat{\theta}$ the parameters vector at the maximum likelihood, and $p_D = \overline{\chi_{\mathrm{eff}}^2(\theta)} - \chi_{\mathrm{eff}}^2(\hat{\theta})$, where the bar denotes the average taken over the posterior distribution. The DIC accounts both for the goodness of

---

[2]Notice that the results would change slightly if the reanalysis of Planck data performed in [37] was used instead of the 2015 release. This data set would lower the significance of the discordance between KiDS and Planck results, although not affecting the considerations made in this paper.
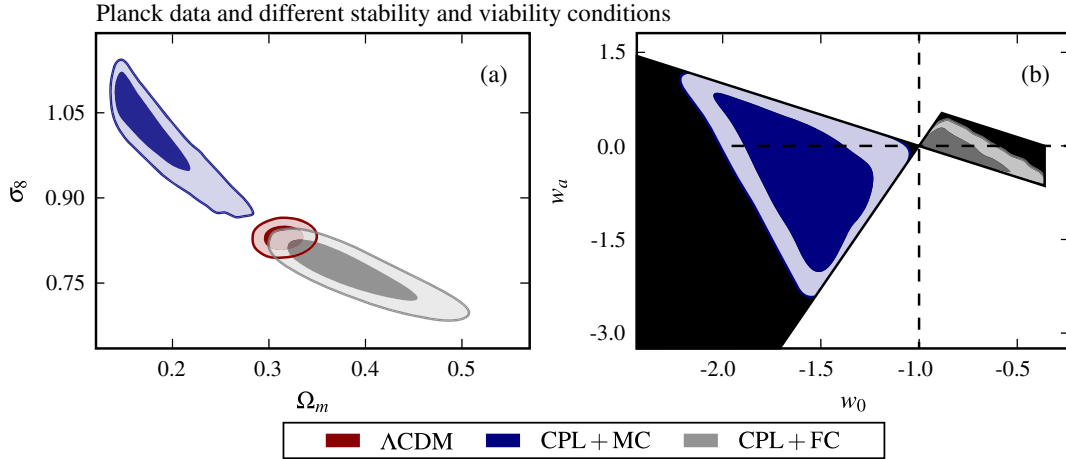
FIG. 2.   The joint marginalized posterior of Ω_m and σ_8 (panel a) and w_0 and w_a (panel b) as obtained with the Planck data in ΛCDM (red contours), CPL with MC (blue contours), and with FC (gray contours). The darker and lighter shades correspond, respectively, to the 68% C.L. and the 95% C.L. regions. The dashed line indicates the point corresponding to the ΛCDM model in the $w_0 - w_a$ plane.

fit through $\chi^2_{\mathrm{eff}}(\hat{\theta})$ and for the Bayesian complexity of the model, p_D, which disfavors more complex models. When comparing ΛCDM with its extension (ext), we compute

$$\Delta \mathrm{DIC} = \mathrm{DIC_{ext}} - \mathrm{DIC_{\Lambda CDM}}. \qquad (4)$$

From this definition, it follows that a negative ΔDIC would support the extended model, while a positive one would support ΛCDM. Finally, we exploit the DIC to assess the concordance of the two different data sets as [7]

$$\log \mathcal{I} = -\frac{\mathcal{G}(P, K)}{2}, \qquad (5)$$

with $\mathcal{G}$ defined as

$$\mathcal{G}(P, K) \equiv \mathrm{DIC}(P \cup K) - \mathrm{DIC}(P) - \mathrm{DIC}(K), \qquad (6)$$

where $P \cup K$ denotes the combination of Planck and KiDS data sets.

IV. RESULTS

In this section, we report the results obtained with the analysis described in Sec. III. We do not report the results on all the cosmological parameters, but rather focus on the quantities introduced above to quantify the tension between the data sets and to assess the effects of the theoretical conditions on it.

The left panel of Fig. 2 shows the constraints obtained in the $\sigma_8 - \Omega_m$ plane analyzing Planck data assuming ΛCDM
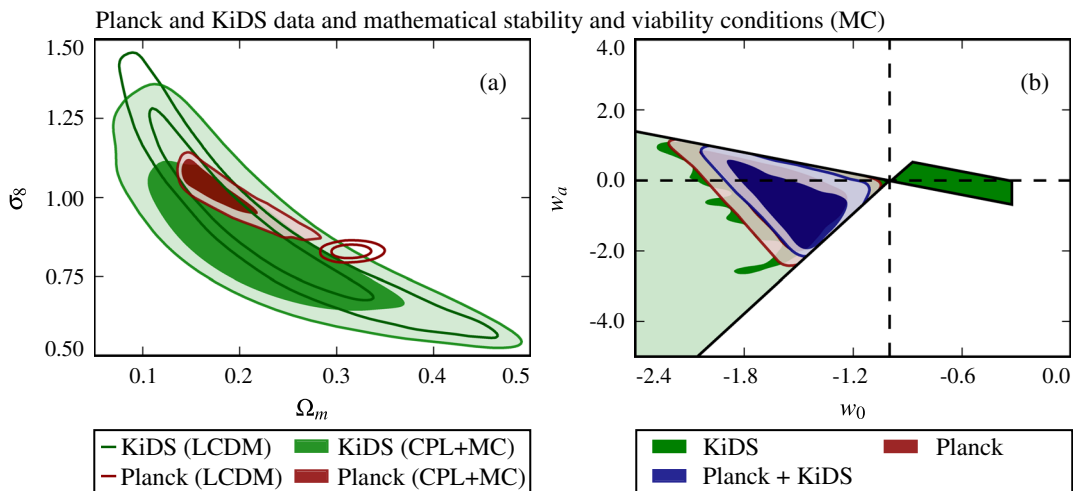

FIG. 3.   The joint marginalized posterior of Ω_m and σ_8 (panel a) and w_0 and w_a (panel b) as obtained analyzing KiDS (green contours) and Planck (red contours) data. Filled contours refer to constraints obtained in CPL with MC, while empty contours (left panel only) refer to ΛCDM constraints. The darker and lighter shades correspond, respectively, to the 68% C.L. and the 95% C.L. regions. The dashed line indicates the point corresponding to the ΛCDM model in the $w_0 - w_a$ plane.

TABLE I.   Tension (T) and concordance ($\log \mathcal{I}$) parameters between KiDS and Planck data in ΛCDM and in CPL with MC and with FC.

	$T(S_8)$	$\log \mathcal{I}$
ΛCDM	2.3σ	-0.48
CPL + MC	1.0σ	0.97
CPL + FC	1.3σ	-0.76

TABLE II.   Model comparison through the obtained values of $\Delta\chi^2_{\rm eff}$ and ΔDIC using as a reference $\chi^2_{\rm eff}$ the one obtained in a ΛCDM analysis.

	$\Delta\chi^2_{\rm eff}$	ΔDIC
CPL + MC		
KiDS	-0.02	3.2
Planck	-2.9	-2.0
Planck + KiDS	-5.4	-5.4
CPL + FC		
KiDS	-0.3	0.2
Planck	1.6	3.2
Planck + KiDS	1.0	4.6

and CPL quintessence with the two possible conditions applied to the model.

We notice that applying MC qualitatively preserves the behavior of the CPL analysis with the PPF approach [8], allowing for smaller values of Ω_m. Adopting the FC instead, moves the contours toward higher Ω_m values. This difference is due to the change in the allowed $w_{\rm DE}$ values, as can be seen in the right panel of Fig. 2. The analysis with MC disfavors the $w_{\rm DE} > -1.0$ region, while the analysis with FC is constrained to be in the $w_{\rm DE} > -1.0$ region. Secondly, we

see that the FC are much more effective in constraining the w_a parameter as the geometric degeneracy between w_0 and w_a is broken by viability conditions. This leads to tighter constraints also in the $\sigma_8 - \Omega_m$ plane.

Given this behavior, we expect the CPL quintessence, with MC, to preserve the ability to ease the tension between Planck and KiDS data. This is indeed the case, as can be seen in the left panel of Fig. 3 and from Table I. Following the hierarchy discussed in [8], the values $T(S_8) = 1$ and $\log \mathcal{I} = 0.97$ highlight how the tension is removed, and the two data sets are now in substantial concordance. The right panel of Fig. 3 shows the constraints on w_0 and w_a. Notice that when the two data sets are combined a deviation of more than 2σ from the ΛCDM model is found. Computing then ΔDIC results in a moderate preference of the data for the CPL model when combining Planck and KiDS (see Table II). As expected, these results are in agreement with those obtained using a PPF approach [8].

The left panel of Fig. 4 shows instead the constraints achieved when FC are used in the analysis. As discussed above, in this case, the Planck data prefer higher values of Ω_m. Even though the tension with KiDS data on the S_8 parameter is eased with respect to the ΛCDM case $[T(S_8) = 1.3]$, the concordance between the two data sets is worsened ($\log \mathcal{I} = -0.76$). As shown in the right panel of Fig. 4, in this case, the constraints on w_0 and w_a are compatible with ΛCDM $w = -1$; additionally, as can be seen in Table II, the CPL model is disfavored with respect to ΛCDM when we account for FC (ΔDIC = 4.6 when the two data sets are combined) because the fit does not improve significantly over the ΛCDM one while the parameter space dimension grows. This is due to the fact that the $w(z) < -1.0$ region, which is the one favored by the data in PPF and MC analysis, is here completely
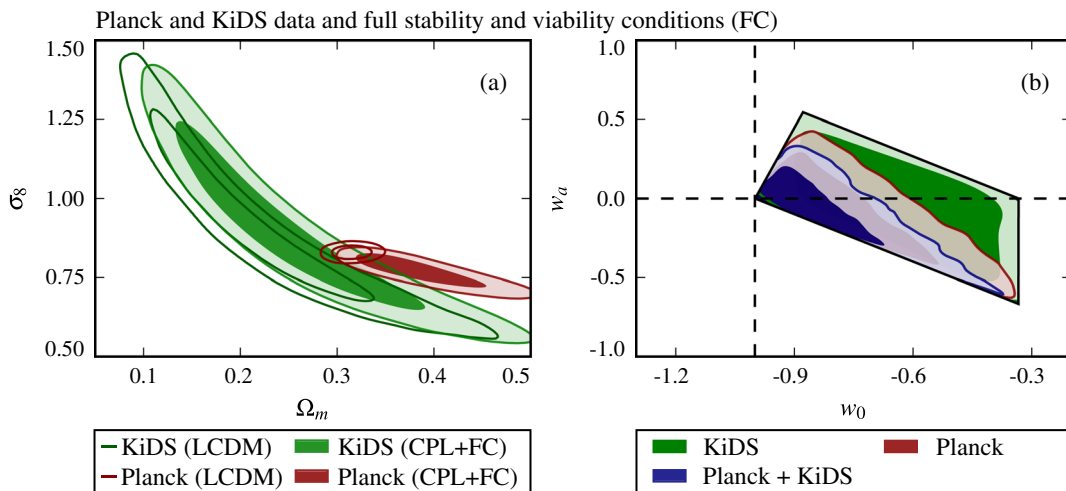

FIG. 4.   The joint marginalized posterior of Ω_m and σ_8 (panel a) and w_0 and w_a (panel b) as obtained analyzing KiDS (red contours) and Planck (blue contours) data. Filled contours refer to constraints obtained in CPL with FC, while empty contours (left panel only) refer to ΛCDM constraints. The darker and lighter shades correspond, respectively, to the 68% C.L. and the 95% C.L. regions. The dashed line indicates the point corresponding to the ΛCDM model in the $w_0 - w_a$ plane.

removed by the FC, as physically viable single field quintessence models are not able to reproduce this evolution.

V. CONCLUSIONS

In this work, we revisited the interesting possibility of easing the tension between weak lensing and CMB data with a dynamical dark energy, whose equation of state is described by the CPL parametrization, in light of the results of [8]. In particular, we explored whether the model favored by Planck and KiDS data in [8] could correspond to a theoretically viable single field quintessence, by restricting the parameter space of CPL to that corresponding to *stable standard quintessence*. With the latter, we indicate DE models corresponding to one scalar field minimally coupled to gravity and without higher order derivative operators. This theoretical assumption leads to restrictions on the allowed parameter space of the CPL parametrization, as described in Sec. II. In order to study the impact of these conditions on the observational constraints, we performed an analysis analogous to the one done in [8], using the theoretical conditions of stability and viability built-in in EFTCAMB.

We considered two types of conditions: mathematical (MC) and the physical stability conditions (PC). The former are rather generic and consider only the numerical stability of the model, without any theoretical consideration. The latter are more restrictive, ruling out all models with ghost or gradient instabilities on the basis of theoretical considerations [20,24]. One convenient way to compare these two classes of conditions is to look at the corresponding parameter space in the (w_0, w_a) plane. While MC allow for the phantom divide crossing, the full set, FC, strictly forbids the region corresponding to $w < -1$, since for smooth single field quintessence ghost instabilities would develop. These instabilities could be avoided with the inclusion of higher order derivative operators or additional degrees of freedom in the dark sector, but in both cases, we would move away from single field, relatively smooth quintessence [20,22].

After performing a fit to KiDS and Planck data by means of EFTCOSMOMC, we find that in the MC case, even though the allowed parameter space is shrunk with respect to the PPF case, the expansion history found in [8] and able to ease the S_8 tension is still allowed by the implemented conditions. Therefore, CPL under MC conditions in our implementation yields results analogous to the general PPF case. In

particular, we find $\Delta DIC = -5.4$, showing a moderate preference of the data for the model. Interestingly, the result changes when we apply the FC: in this case, the parameter space of CPL is significantly reduced and both KiDS and Planck contours move towards higher values of Ω_m, as shown in Fig. 2, with the net effect of decreasing the tension parameter to $T(S_8) = 1.3\sigma$. However, the value of $\Delta DIC = 4.6$ (for Planck + KiDS) shows that the model is disfavored with respect to ΛCDM.

In conclusion, as expected, the CPL expansion history favored by Planck + KiDS data per [8], cannot correspond to stable single field quintessence, and this is shown very clearly by the contours in Fig. 4, where we plot the outcome of our analysis including stability conditions. The best fit model of [8] shall rather be interpreted in terms of multiple fields scenarios, with the DE d.o.f. remaining relatively smooth with respect to dark matter. The results we obtained highlight how parametrized approaches to ΛCDM extensions, although extremely useful to agnostically explore departures from the standard cosmological model, need to be complemented with theoretically priors if one wants to connect the results to viable models of DE. Our method allows us to quantify the tension between data sets and the preference of models while restricting to specific classes of models in a statistically meaningful way. In this case, we find that, if one indeed restricts to standard quintessence and invokes conditions of theoretical stability, ΛCDM remains a better fit to the data. We leave for future work the exploration of the tension between Planck and KiDS data sets in more general models of dark energy, e.g., stable and viable Horndeski models.

[1] T. D. Kitching *et al.* (CFHTLenS Collaboration), Mon. Not. R. Astron. Soc. **442**, 1326 (2014).

[2] H. Hildebrandt *et al.*, Mon. Not. R. Astron. Soc. **465**, 1454 (2017).

[3] R. Adam *et al.* (Planck Collaboration), Astron. Astrophys. **594**, A1 (2016).

[4] M. Raveri, Phys. Rev. D **93**, 043522 (2016).

[5] S. Seehars, S. Grandis, A. Amara, and A. Refregier, Phys. Rev. D **93**, 103507 (2016).

[6] S. Grandis, S. Seehars, A. Refregier, A. Amara, and A. Nicola, J. Cosmol. Astropart. Phys. 05 (2016) 034.

[7] S. Joudaki *et al.*, Mon. Not. R. Astron. Soc. **465**, 2033 (2017).

[8] S. Joudaki *et al.*, Mon. Not. R. Astron. Soc. **471**, 1259 (2017).

[9] N. Aghanim *et al.* (Planck Collaboration), Astron. Astrophys. **594**, A11 (2016).

[10] F. Khlinger *et al.*, arXiv:1706.02892.

[11] E. van Uitert *et al.*, arXiv:1706.05004.

[12] J. Hamann and J. Hasenkamp, J. Cosmol. Astropart. Phys. 10 (2013) 044.

[13] E. Di Valentino, A. Melchiorri, and J. Silk, Phys. Rev. D **92**, 121302 (2015).

[14] D. J. E. Marsh, P. Bull, P. G. Ferreira, and A. Pontzen, Phys. Rev. D **90**, 105023 (2014).

[15] M. Chevallier and D. Polarski, Int. J. Mod. Phys. D **10**, 213 (2001).

[16] E. V. Linder, Phys. Rev. Lett. **90**, 091301 (2003).

[17] W. Hu and I. Sawicki, Phys. Rev. D **76**, 104043 (2007).

[18] W. Hu, Phys. Rev. D **77**, 103524 (2008).

[19] W. Fang, W. Hu, and A. Lewis, Phys. Rev. D **78**, 087303 (2008).

[20] P. Creminelli, G. D'Amico, J. Noreña, and F. Vernizzi, J. Cosmol. Astropart. Phys. 02 (2009) 018.

[21] A. Vikman, Phys. Rev. D **71**, 023515 (2005).

[22] W. Hu, Phys. Rev. D **71**, 047301 (2005).

[23] R. R. Caldwell and M. Doran, Phys. Rev. D **72**, 043527 (2005).

[24] S. M. Carroll, M. Hoffman, and M. Trodden, Phys. Rev. D **68**, 023509 (2003).

[25] S. M. Carroll, A. D. Felice, and M. Trodden, Phys. Rev. D **71**, 023525 (2005).

[26] D. A. Easson and A. Vikman, arXiv:1607.00996.

[27] C. Deffayet, O. Pujolas, I. Sawicki, and A. Vikman, J. Cosmol. Astropart. Phys. 10 (2010) 026.

[28] W. Hu, Phys. Rev. D **71**, 047301 (2005).

[29] Z.-K. Guo, Y.-S. Piao, X.-M. Zhang, and Y.-Z. Zhang, Phys. Lett. B **608**, 177 (2005).

[30] B. Hu, M. Raveri, N. Frusciante, and A. Silvestri, Phys. Rev. D **89**, 103530 (2014).

[31] M. Raveri, B. Hu, N. Frusciante, and A. Silvestri, Phys. Rev. D **90**, 043513 (2014).

[32] N. Frusciante, G. Papadomanolakis, and A. Silvestri, J. Cosmol. Astropart. Phys. 07 (2016) 018.

[33] J. T. A. de Jong, G. A. Verdoes Kleijn, K. H. Kuijken, and E. A. Valentijn, Exp. Astron. **35**, 25 (2013).

[34] K. Kuijken *et al.*, Mon. Not. R. Astron. Soc. **454**, 3500 (2015).

[35] A. J. Mead, J. A. Peacock, C. Heymans, S. Joudaki, and A. F. Heavens, Mon. Not. R. Astron. Soc. **454**, 1958 (2015).

[36] P. A. R. Ade *et al.* (Planck Collaboration), Astron. Astrophys. **594**, A13 (2016).

[37] N. Aghanim *et al.* (Planck Collaboration), Astron. Astrophys. **596**, A107 (2016).

[38] A. Lewis, A. Challinor, and A. Lasenby, Astrophys. J. **538**, 473 (2000).

[39] A. Lewis and S. Bridle, Phys. Rev. D **66**, 103511 (2002).

[40] D. J. Spiegelhalter, N. G. Best, B. P. Carlin, and A. van der Linde, J. R. Stat. Soc. Ser. B **76**, 485 (2014).